Biology of Reproduction, 2022, 1–11
https://doi.org/10.1093/biolre/ioac189
Research Article

Luteinizing hormone receptor promotes angiogenesis in ovarian endothelial cells of *Macaca fascicularis* and *Homo sapiens*†

Merete Lund, Andrew C. Pearson*, Megan A.G. Sage and Diane M. Duffy*

Department of Physiological Sciences, Eastern Virginia Medical School, Norfolk, Virginia, USA

***Correspondence:** Department of Physiological Sciences, Eastern Virginia Medical School, Norfolk, VA, USA, PO Box 1980; Norfolk, VA 23501-1980, USA. E-mail: duffydm@evms.edu; E-mail: pearsoac@evms.edu

†**Grant Support:** This research was supported by the Eunice Kennedy Shriver National Institute of Child Health and Human Development (grants HD071875 and HD097675 to DMD).

Abstract

Angiogenesis within the ovarian follicle is an important component of ovulation. New capillary growth is initiated by the ovulatory surge of luteinizing hormone (LH), and angiogenesis is well underway at the time of follicle rupture. LH-stimulated follicular production of vascular growth factors has been shown to promote new capillary formation in the ovulatory follicle. The possibility that LH acts directly on ovarian endothelial cells to promote ovulatory angiogenesis has not been addressed. For these studies, ovaries containing ovulatory follicles were obtained from cynomolgus macaques and used for histological examination of ovarian vascular endothelial cells, and monkey ovarian microvascular endothelial cells (mOMECs) were enriched from ovulatory follicles for in vitro studies. mOMECs expressed LHCGR mRNA and protein, and immunostaining confirmed LHCGR protein in endothelial cells of ovulatory follicles in vivo. Human chorionic gonadotropin (hCG), a ligand for LHCGR, increased mOMEC proliferation, migration and capillary-like sprout formation in vitro. Treatment of mOMECs with hCG increased cAMP, a common intracellular signal generated by LHCGR activation. The cAMP analog dibutyryl cAMP increased mOMEC proliferation in the absence of hCG. Both the protein kinase A (PKA) inhibitor H89 and the phospholipase C (PLC) inhibitor U73122 blocked hCG-stimulated mOMEC proliferation, suggesting that multiple G-proteins may mediate LHCGR action. Human ovarian microvascular endothelial cells (hOMECs) enriched from ovarian aspirates obtained from healthy oocyte donors also expressed *LHCGR*. hOMECs also migrated and proliferated in response to hCG. Overall, these findings indicate that the LH surge may directly activate ovarian endothelial cells to stimulate angiogenesis of the ovulatory follicle.

Summary Sentence The ovulatory surge of LH may regulate follicular angiogenesis by acting directly at LHCGRs on ovarian vascular endothelial cells.

Graphical Abstract

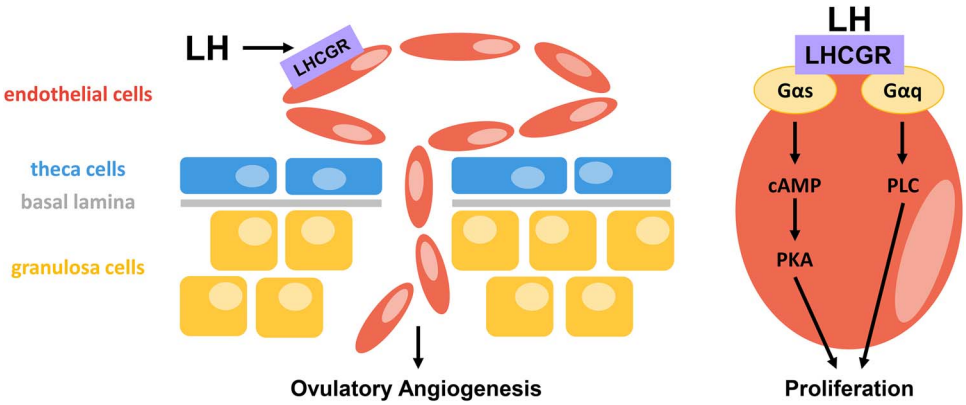

Keywords: ovary, ovulation, LHCGR, gonadotropin, monkey, human

Introduction

Ovulation can be defined as rupture of the ovarian follicle to release a mature oocyte [1]. Vascular changes associated with ovulation include follicular angiogenesis, increased vascular permeability, and increased follicular blood flow; these vascular changes have been associated with successful ovulation [1]. Ovulation is initiated by the midcycle surge of luteinizing hormone (LH), and ovulatory vascular changes can be mediated within the follicle by LH-stimulated paracrine factors [2]. LH has been shown to regulate follicular production of many angiogenic factors, including progesterone

Received: March 29, 2022. **Revised:** August 26, 2022. **Accepted:** October 4, 2022

[3, 4], prostaglandin E2 (PGE2, [5, 6]), vascular endothelial growth factor A (VEGFA, [7–9]), placental growth factor (PGF, [8]), thrombospondins (THBS1-4, [10, 11]), and angiopoietins (ANG1, ANG2, [7, 12]). Each of these vascular regulators has been implicated in angiogenesis of the ovulatory follicle and/or young corpus luteum. However, a direct angiogenic action of LH on ovarian vascular endothelial cells to initiate and regulate ovulatory changes in the vasculature has not been explored.

LH acts via its receptor, LHCGR, which is activated by both LH and human chorionic gonadotropin (hCG). LHCGR mRNA and protein are expressed by multiple cell types within the ovulatory follicle [13–15]. Primary targets for LH and hCG action include granulosa cells and theca cells, although very low levels of LHCGR mRNA and protein have been detected in cumulus cells and oocytes [13, 14]. LHCGR expression by and LH/hCG action at ovarian vascular endothelial cells has not been reported, but LHCGR mRNA and protein have been reported on vascular endothelial cells of non-gonadal blood vessels [16–19]. In the present study, microvascular endothelial cells obtained from ovulatory follicles of cynomolgus macaques and women were used to determine if there is a potential role of endothelial cell LHCGR in follicular angiogenesis associated with ovulation.

Methods

Animals

Whole ovaries and ovarian biopsies were obtained from 4- to 8-year-old female cynomolgus macaques (*Macaca fascicularis*) at Eastern Virginia Medical School (EVMS, Norfolk, VA). All animal protocols were conducted in accordance with the National Institutes of Health's Guide for the Care and Use of Laboratory Animals and were approved by the EVMS Animal Care and Use Committee and were performed as described previously [20]. Utilizing chemical restraint (ketamine, 5–10 mg/kg body weight), blood samples were obtained as needed by femoral venipuncture and serum was stored at −20°C. The Immulite 1000 immunoassay system (Siemens Medical Diagnostics Solutions, Rockville, MD) was used to determine serum estradiol and progesterone levels. Aseptic surgeries were performed by laparotomy under isoflurane anesthesia. Postoperative analgesia was accomplished with buprenorphine and a non-steroidal anti-inflammatory drug (ketoprofen or meloxicam). Monkey corpus luteum and adrenal were obtained at necropsy, fixed, and sectioned as described for ovaries below.

Ovarian stimulation

The ovarian stimulation protocol has been previously described [20]. Monkeys received 90 IU of recombinant human follicle-stimulating hormone (FSH, Organon, Jersey City, NJ) for 6–8 days, then 90 IU of FSH plus 60 IU of recombinant human LH (Serono Reproductive Biology Institute, Rockland, MA) for 2 days to stimulate the growth of multiple follicles. A GnRH antagonist (0.03 mg/kg Ganirelix; Organon) was also administered daily to prevent an endogenous LH surge. Ultrasonography and rising serum estradiol were used to monitor follicle growth. Follicle aspiration was performed during aseptic surgery before (0 h) or up to 36 h after 1000 IU recombinant hCG (Serono) administration. At surgery, each follicle with a diameter greater than 4 mm was pierced and aspirated with a 22-gauge needle. All aspirates from a single animal were pooled and used for the enrichment of granulosa cells as previously described [20] or for obtaining ovarian microvascular endothelial cells (below). Whole ovaries were also obtained from monkeys experiencing ovarian stimulation. Some ovaries were used for obtaining ovarian microvascular endothelial cells (below). Additional ovaries were bisected, maintaining at least two follicles greater than 4 mm in diameter on each piece, fixed in 10% formalin, and embedded in paraffin for sectioning. For each experiment using monkey ovaries or granulosa cells, *n* reflects the total number of tissues or aspirates, each collected from a different animal.

Monkey ovarian microvascular endothelial cells

Monkey ovarian microvascular endothelial cells (mOMECs) were enriched from either whole stimulated monkey ovaries [5] or follicular aspirates after oocyte removal [21], as previously described. All mOMEC lines were tested as described by Trau et al. [5] to ensure a >95% endothelial cell phenotype. For these experiments, mOMECs (passages 4–9) were plated on fibronectin-coated culture ware and maintained in EGM-2MV (EGM2) growth media (Lonza, Salisbury, MD). mOMECs were cultured in serum- and growth factor free media (EMB-2 (basal); Lonza) containing 1% fetal bovine serum overnight prior to experiments described below. For each experiment using mOMECs, *n* reflects the number of distinct mOMEC lines, each enriched from a different animal.

Monkey theca cells

Monkey theca cells were isolated from ovarian follicles and characterized as previously described [22]. Theca cells were maintained in a humidified cell culture incubator at 37°C in an atmosphere of 5% O_2, 5% CO_2, 90% N_2. Theca cell base media was a pH 7.4, 1:1 mixture of low glucose DMEM (Sigma), and Ham's F-12 medium (Sigma) supplemented with 5.96 g/L HEPES (Sigma), 2.4 g/L NaHCO3 (Sigma), 3.33 mU/mL insulin (Humulin R U-100, Lilly), 20 nM selenium (Sigma), 1 μM vitamin E (Sigma), and antibiotic/antimycotic mixture (Sigma) [23]. For these experiments, theca cells (passages 3–5) were plated on fibronectin-coated culture ware and maintained in growth media, which was base media plus 10% fetal bovine serum (R&D Systems), 10% horse serum (Gibco), and 2% UltroSer G (PALL Life Sciences) [23]. Theca cells were cultured in serum-free media [23] for 24 h before use in experiments and during experimental treatments. Serum-free medium was base media plus 1.0 mg/mL bovine serum albumin (Sigma) and 100 μg/mL apo-transferrin (Sigma). For each experiment using theca cells, *n* reflects the number of distinct primary theca cell lines, each enriched from a different animal.

Human ovarian microvascular endothelial cells

Human ovarian microvascular endothelial cells (hOMECs) were enriched from follicular aspirates obtained during oocyte retrieval from healthy young women undergoing ovarian stimulation for oocyte donation at the Jones Institute for Reproductive Medicine, EVMS. This use of discarded human follicular aspirates does not constitute human subjects research as determined by the EVMS Institutional Review Board. hOMECs were enriched as previously described [21]. Culture, characterization, and experiments were performed as

described for mOMECs. For each experiment using hOMECs, *n* reflects the number of distinct primary hOMEC cell lines, each enriched from a different woman.

Immunohistochemistry

Immunostaining using paraffin-embedded monkey tissues sectioned at 5 μm has been previously described [5]. Tissue sections were heated to 55°C and deparaffinized. mOMECs, hOMECs, theca cells, and granulosa cells were cultured on fibronectin-coated chamber slides (Tissue-Tek, Thermofisher, Waltham, MA) and fixed in 10% formalin for 20 min. For immunodetection of LHCGR, slides were exposed to basic antigen retrieval (heating to 85–90°C for 30 min in 10 mM Tris, 1.3 mM EDTA, 0.05% Tween 20). Slides were blocked in phosphate-buffered saline (PBS) + 0.1% Triton X-100 containing either 0.75% non-immune serum (LHCGR) or 5% non-immune serum (VWF, CYP17A1, CYP19A1). Slides were then incubated overnight in a humidified chamber at 4°C with a primary antibody against LHCGR (1:200, gift of Dr. Asgerally Fazleabas, Michigan State University, [24]), VWF (1:200, rrid: AB_2315602; Dako, Glostrup, Denmark), CYP17A1 (0.35 μg/mL; product #14447-1-AP, Proteintech, Rosemont, IL), or CYP19A1 (1:200, Serotec, Raleigh, NC) in PBS–Triton. Tissues were color-developed by using a rabbit (LHCGR, VWF, CYP17A1) or mouse (CYP19A1) Vectastain ABC kit (Vector Laboratories, Burlingame, CA) and DAB kit (Vector) according to protocols provided by the manufacturer. Slides were counterstained in hematoxylin, dehydrated, and permanently coverslipped. Images were obtained using an Olympus BX41 microscope fitted with a DP70 digital camera and associated software. Omission of the primary antibody served as a negative control.

PCR amplification

Total RNA was prepared using Trizol reagent (Invitrogen, Waltham, MA), treated with DNase, and reverse transcribed using an oligo-dT primer and moloney murine leukemia virus reverse transcriptase (M-MLV RT) as previously described [25, 26]. Quantitative PCR (qPCR) was performed using a Roche LightCycler and FastStart DNA Master SYBR Green I kit (Roche Diagnostics, Indianapolis, IN). The strategy for design of species-specific primers for qPCR of cynomolgus macaque mRNAs and establishment of reaction conditions was previously described [25]. Monkey and human cDNA was used as a template for qPCR of *LHCGR* (forward: GTTGATTCCCAAACCAAGG; reverse: GGCCACCACATTGAGA; Accession numbers XM_005575920 (monkey) and NM_000233 (human); 363 base pair product). PCR products span an intron/exon boundary to avoid undetected amplification of genomic DNA and sequencing confirmed amplicon identity. At least five log dilutions of the sequenced PCR product were included in each assay and used to generate a standard curve. No amplification was observed when cDNA was omitted. For each sample, the content of the mRNA of interest was determined in independent assays. Numerical data are expressed as the ratio of mRNA of interest to *ACTB* [25].

Nested PCR for *LHCGR* was performed using 1 μL of reaction product from the first round amplification as described above with a primer pair (forward: TGTCTACACCCTCACCGTCA; reverse: ATTGCTGACACCCACAAGGG; 163 base pair product), which were located internal to the original primer pair (above). The product of the second round of PCR was separated on a 2% agarose gel, photographed under ultraviolet illumination, and sequenced to confirm identity.

Media cAMP

mOMECs and hOMECs were cultured for 24 h without (basal) or with hCG (Sigma-Aldrich, St. Louis, MO) at concentrations of 0.2, 2.0, or 20 IU/mL media, PGE_2 (1 μM; Cayman Chemical, Ann Arbor, MI), or LH (20 or 200 IU/mL; Serono). Cell culture media samples were centrifuged to pellet any cells, and the supernatant was stored at −20°C. Media samples were analyzed utilizing a cAMP enzyme-linked immunosorbent assay (ELISA) (#581001; Cayman Chemical) according to kit instructions for acetylation. Levels of media cAMP were normalized to the protein content of the corresponding cell lysates, as determined by the bicinchoninic acid method (Sigma). Inter-assay coefficient of variation (CV) was 11.2% and the intra-assay CV was 11.6%.

Angiogenesis assays

Migration was assessed as previously described [5]. Briefly, mOMECs or hOMECs were trypsinized and immediately added to fibronectin-coated six-well membrane inserts with 8-μm pores (BD Biosciences, San Jose, CA) in basal media; media in the lower chamber consisted of either basal media alone or with hCG (20 IU/mL). After 24 h in a standard cell culture incubator, a cotton swab was used to gently remove non-migrated cells from the upper surface of the membrane. Membranes were fixed in 70% ethanol and stained with hematoxylin and eosin. Images of five different fields were taken of the membrane side opposite to the side of plating, and migrated cells were counted. The average number of migrated cells/image was 25. The average number of migrated cells was determined for each treatment group.

To assess proliferation, mOMECs or hOMECs were grown to 60% confluence on chamber slides as previously described [5]. Cells were cultured for 24 h in basal media with or without the addition of hCG (20 IU/mL), LH (20 or 200 IU/mL), H-89 (1 μM; Sigma #19-141), U71322 (1 μM; Sigma #U6756), GF109203X (1 μM; Tocris #0741), SB203580 (20 μM; Sigma #559395), U0126 (10 μM; Sigma #U012), or dibutyryl cAMP (10 μM; Sigma #D0627). Cells were fixed in 10% formalin for 20 min, then immunostained for Ki67 as described above with no antigen retrieval using a mouse monoclonal antibody (1:100 dilution, Dako) and mouse Vectastain ABC kit (Vector). For each mOMEC line, images of five different fields were obtained for each treatment. Positive and negative nuclei were counted, with a minimum of 40 cells scored per image. The percentage of Ki67 positive nuclei out of total nuclei was then determined for each treatment group.

To assess capillary-like sprout formation in vitro, Cytodex microcarrier beads (GE Healthcare, Little Chalfont, UK) were incubated with mOMECs (250–500 cells per bead) and embedded in a three-dimensional fibrin matrix, as previously described [5]. Basal media without or with 20 IU/mL hCG was added on top of each matrix. Five beads in each well were photographed at the start of culture (day 0), day 1, and day 2 of culture using an Olympus CK40 microscope, Infinity Lite camera, and associated software (Lumenera, Nepean, ON, Canada). For each bead imaged, the number of sprouts and length of each sprout was determined for each day. An average number of sprouts and average length of sprouts was determined for each treatment group on each day of culture.

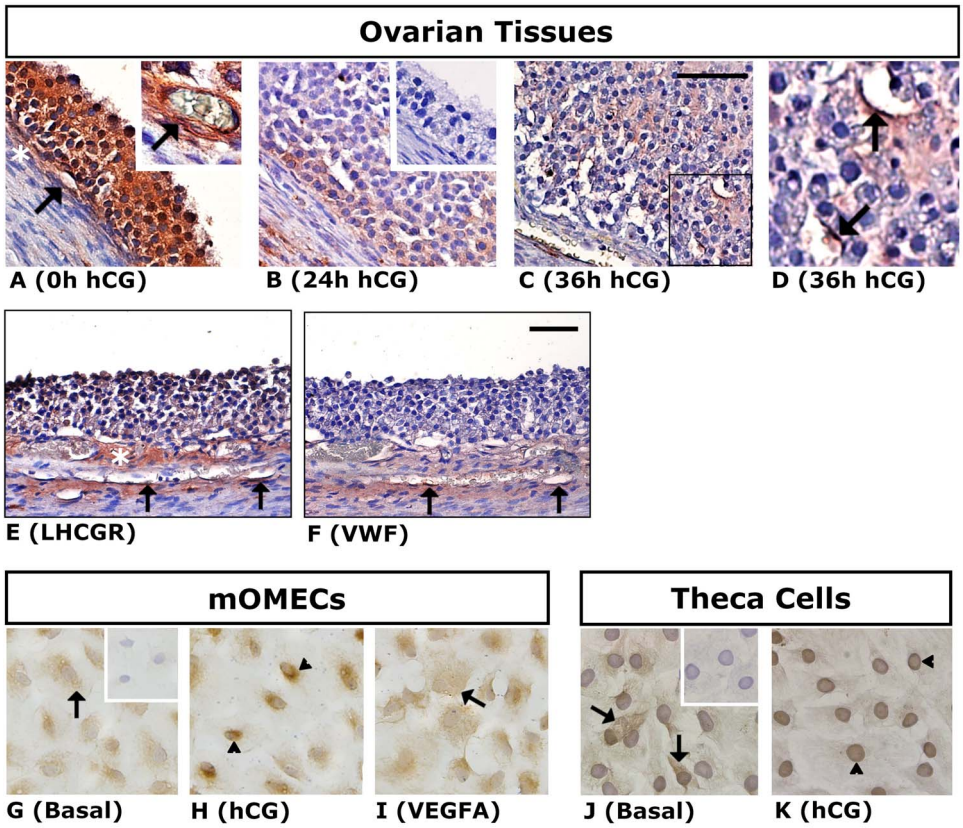

Figure 1. LHCGR immunodetection in monkey ovarian tissues and cells. LHCGR immunodetection (brown) in monkey ovarian follicles after ovarian stimulation before hCG (0 h hCG, A and A inset), 24 h after hCG (B), and 36 h after hCG administration (C, D). (D) shows an enlargement of indicated area in (C). In (A)–(D), arrows indicate putative endothelial cells, surrounding red blood cells in small vessels. Asterisk (*) indicates ovarian stroma consistent with location of theca cells. In (A)–(C), follicle antrum is upper right, granulosa are cells central, and ovarian stroma is lower left. (A)–(C) use bar in (C) = 40 μm. (A) inset and (D) are 2.5× higher magnification than (A)–(C). LHCGR (E) and VWF (F) localization by immunostaining in adjacent monkey ovarian tissue sections obtained 0 h after hCG. Arrows indicate endothelial cells of a perifollicular vessel; asterisk (*) indicates ovarian stroma consistent with location of theca cells. In (E)–(F), follicle antrum is on the top, granulosa cells are central, and ovarian stroma is at the bottom of the image. (E)–(F) use bar in (F) = 40 μm. Images are representative of $n = 4$–7 monkey ovarian tissues per treatment group. (G)–(I) LHCGR immunodetection in mOMECs cultured with basal medium (G), hCG (H), or VEGFA (I). (J)–(K) show LHCGR immunodetection in monkey theca cells in vitro after culture without (J) or with (K) hCG. For (G)–(K), arrows indicate LHCGR detection across entire cell; arrowheads indicate the concentration of LHCGR detection near the nucleus. Insets in (B), (G), and (J) show the absence of brown staining when the primary antibody was omitted. Images are representative of $n = 4$ mOMEC or theca cell lines per treatment group.

Data analysis

Data were assessed for heterogeneity of variance using Bartlett test. Data were log transformed when Bartlett test yielded $P < 0.05$; log-transformed data were subjected to Bartlett test to confirm that $P > 0.05$. Log transformation was performed for granulosa cell *LHCGR* and cAMP. As indicated in the figure legends, data sets were assessed by two-tail paired *t*-test or ANOVA followed by Duncan multiple range test (StatPak version 4.12 software; Northwest Analytical, Portland, OR). Significance was assumed at $P < 0.05$. Data are expressed as mean + SEM.

Results

Ovarian vascular endothelial cells express LHCGR

To determine if LHCGR is expressed by ovarian endothelial cells, monkey ovarian tissues were used for immunodetection of LHCGR. LHCGR was detected in granulosa cells, with strongest immunodetection in granulosa cells of large antral (preovulatory) follicles before (0 h) hCG administration (Figure 1A). Granulosa cell immunostaining for LHCGR was apparently reduced after hCG (Figure 1B and C). Immunodetection of LHCGR was also present in the ovarian stroma surrounding large antral follicles both before and after hCG administration, consistent with the location of theca cells (Figure 1A; asterisk). In addition, LHCGR was detected in the vascular endothelial cells of these large follicles. Brown staining cells with thin cytoplasm were present surrounding luminal areas containing clusters of red blood cells near the granulosa cell basement membrane before hCG (Figure 1A inset; arrow) and within the luteinizing granulosa cell layer after hCG administration (Figure 1C and D; arrows). Interestingly, hCG administration did not alter the apparent intensity of LHCGR immunodetection in presumptive vascular endothelial cells (compare Figure 1A inset Figure 1D).

To support the identification of LHCGR in ovarian vascular endothelial cells, adjacent monkey ovarian tissue sections were stained for LHCGR (Figure 1E) and VWF, an endothelial cell protein (Figure 1F). Endothelial cells lining a small vessel showed dark brown staining for both LHCGR and VWF (arrows), supporting the detection of LHCGR in follicular endothelial cells in vivo.

To confirm LHCGR detection in ovarian vascular endothelial cells, cultured mOMECs were immunostained for LHCGR (Figure 1G–I). In mOMECs maintained in basal media, brown staining was dispersed across each cell (Figure 1G, arrow), consistent with the anticipated plasma membrane location of LHCGR. Treatment in vitro with hCG prior to immunostaining resulted in the clustering of LHCGR immunodetection near the nucleus in most mOMECs (Figure 1H, arrowheads). Treatment in vitro with VEGFA prior to immunostaining resulted in LHCGR immunodetection dispersed across the cell (Figure 1I, arrow), similar to that seen after culture with basal media only. Isolated monkey theca cells also showed immunodetection of LHCGR using this approach (Figure 1J and K), which served as an additional positive control. LHCGR immunostaining was also observed in the large luteal cells of the corpus luteum obtained on day 7 of the luteal phase (Supplementary Figure S1A), but LHCGR immunodetection was not prominent in endothelial cells of luteal capillaries (Supplementary Figure S1A) or vessels of the ovarian stroma (Supplementary Figure S1B). LHCGR was detected in the zona reticularis of the monkey adrenal, but the adrenal medulla did not show immunodetection of LHCGR (Supplementary Figure S1C).

LHCGR was present in key monkey cells. Granulosa cells aspirated from monkey ovarian follicles before (0 h) and after hCG treatment in vivo also expressed *LHCGR*, with highest levels before hCG and lower levels after hCG administration (Figure 2A). *LHCGR* was also present in cultured monkey theca cells (Figure 2B), detectable by PCR but below the quantitative range of our qPCR assay. *LHCGR* was inconsistently detected in cultured mOMECs using qPCR. A nested PCR approach demonstrated the presence of *LHCGR* in cultured mOMECs, with amplification of *LHCGR* in granulosa cells serving as a positive control (Figure 2C). We considered that *LHCGR* detection in mOMECs may be due to small numbers of contaminating granulosa cells or theca cells. Immunostaining for CYP17A1 (theca cell protein) or CYP19A1 (granulosa cell protein) did not indicate the presence of these cell types in cultured mOMECs (Supplementary Figure S2).

LHCGR stimulation promotes angiogenic events in vitro

Endothelial cell migration, proliferation, and sprout formation are early events in the formation of new capillaries [27]. The LHCGR agonist hCG at a concentration of 20 IU/mL [28] increased mOMEC migration compared with untreated cells (Figure 3A–C). hCG also increased the number of mOMECs immunostaining positive for the proliferation antigen Ki67 (Figure 3D–F). The ability of hCG to modulate capillary sprout formation was also explored in vitro (Figure 3G–M). hCG tended to increase the number of capillary-like sprouts after 1 day in vitro (Figure 3H), with significant increase after 2 days (Figure 3J). hCG did not alter the length of capillary sprouts formed in vitro (Figure 3G and I).

LHCGR signaling pathways in mOMECs

LHCGR is a member of the seven transmembrane family and has been reported to couple to multiple G proteins [29, 30]. mOMECs treated with 20 IU/mL hCG had increased cAMP in culture media; lower hCG concentrations did not increase cAMP (Figure 4A). PGE2, previously shown to

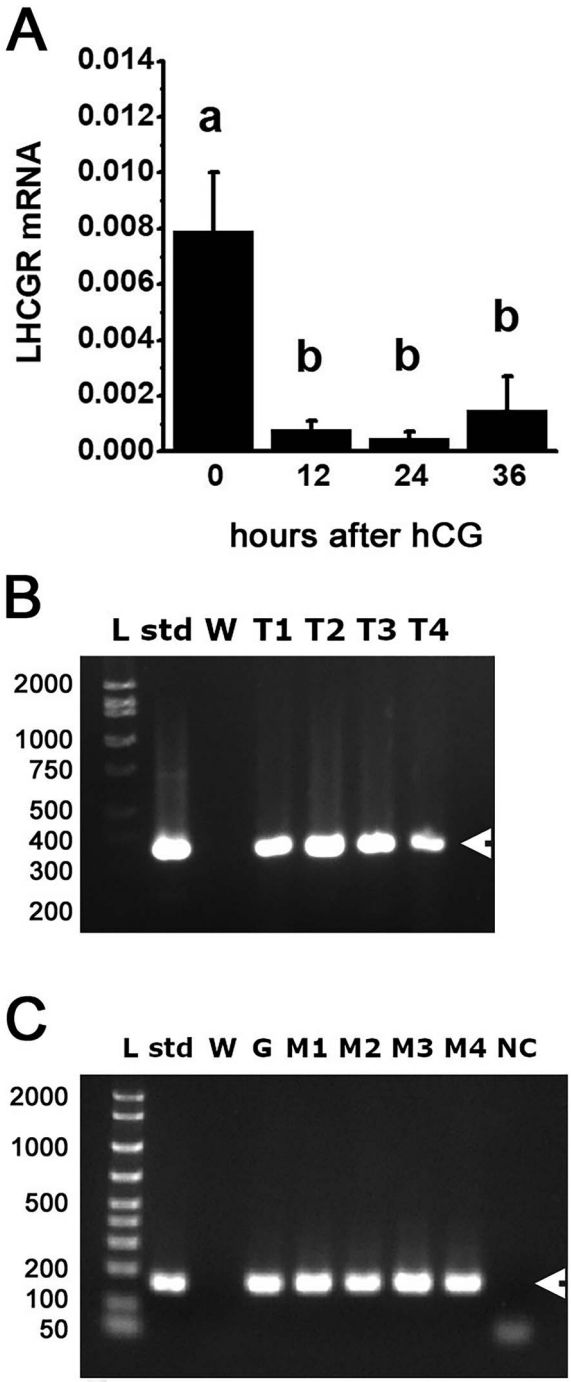

Figure 2. LHCGR mRNA in monkey cells. (A) LHCGR mRNA quantification by qPCR in monkey granulosa cells obtained after ovarian stimulation before hCG (0 h) and 12, 24, or 36 h after hCG administration. LHCGR mRNA copy number is expressed relative to copy number for ACTB mRNA. $N = 4$ animals/group; groups with different letters are different, $P < 0.05$ by ANOVA with one repeated measure. (B) LHCGR mRNA detection by PCR in cultured monkey theca cells. LHCGR cDNA amplified fragment (363 bp) shown at arrow (right). Lanes show the molecular size ladder (L) and amplification of cDNA from LHCGR standard (std), no cDNA control (water; W), and individual monkey theca cell lines (T1–T4; $n = 4$). C. LHCGR mRNA was detected in mOMECs by nested PCR. Nested LHCGR cDNA amplified fragment (163 bp) is shown at arrowhead (right). Sample lanes show the molecular size ladder (L), amplification of cDNA from LHCGR standard (std), no cDNA control (water; W), monkey granulosa cells (G), individual mOMEC lines (M1–M4; $n = 4$), and re-amplified no cDNA control (NC) from the first round PCR.

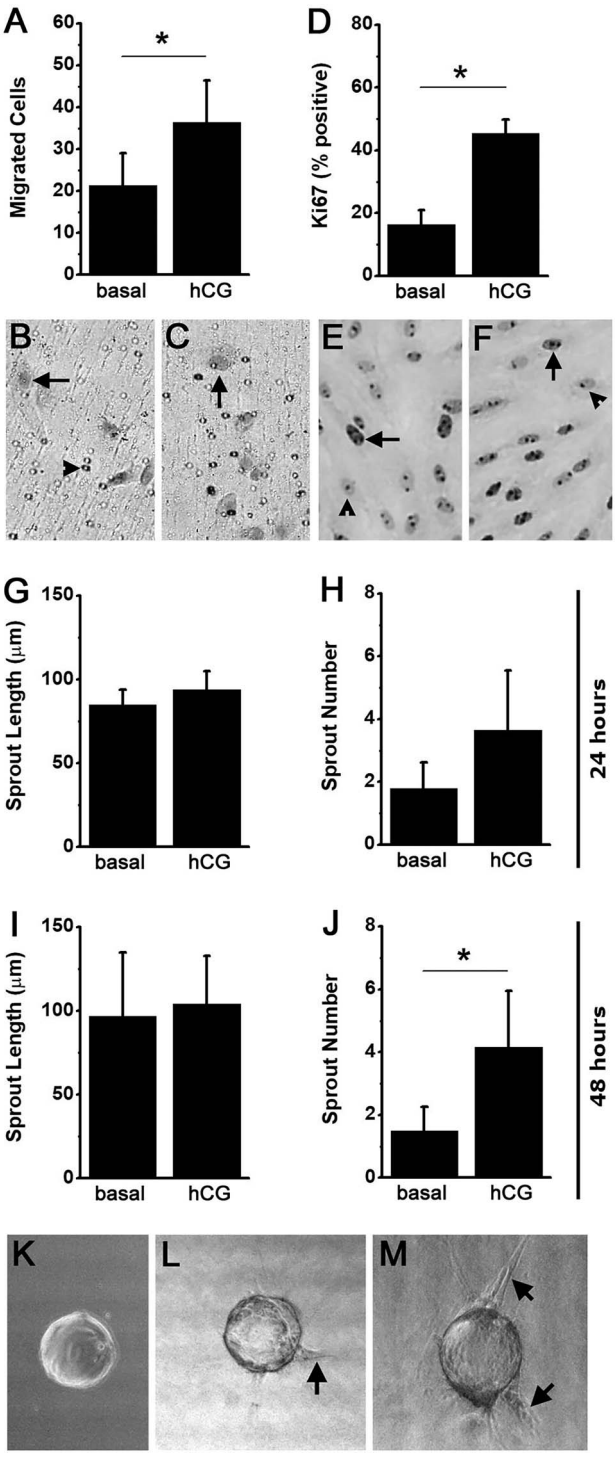

Figure 3. hCG stimulates angiogenic events in mOMECs. (A) hCG increases the number of migrated cells when compared to basal medium alone. (B) (basal) and (C) (hCG) show sections of migration membranes, with arrows indicating migrated cells and arrowhead indicating a pore. $N = 4$ mOMEC lines. (D) hCG increases mOMEC proliferation over basal medium. (E) (basal) and (F) (hCG) show Ki67 staining, with arrows indicating Ki67 positive (dark) cell nuclei and arrowheads indicating Ki67 negative (pale) nuclei; $n = 5$ mOMEC lines. (G)–(J) mOMEC sprout formation in vitro increases with hCG treatment. Sprouts were assessed for sprout length (G, I) and sprout number (H, J) after 1 (G, H) or 2 days (I, J) in vitro. Data in (G)–(J) reflect $n = 5$ mOMEC lines. Representative sprouting is shown for time of plating (day 0; K), basal media on day 2 (L), and hCG treated on day 2 (M); arrows show representative sprouts. In (A), (D), and (J), significant differences were detected by paired *t*-test, $P < 0.05$, as indicated by the asterisk (*).

increase mOMEC cAMP [5], served as a positive control. PGE2 increased cAMP, but the combination of PGE2 and hCG resulted in media cAMP levels similar to either agonist alone (Figure 4B).

To further explore LHCGR signal transduction in mOMECs, cells were treated with signal transduction pathway modulators in vitro, and proliferation was assessed by Ki67 immunodetection. Treatment of mOMECs with dibutyryl cAMP increased proliferation above basal levels, similar to treatment with hCG (Figure 4C). Chemical inhibitors of signal transduction intermediaries were used to block hCG-stimulated proliferation. The protein kinase A inhibitor H89 alone did not alter proliferation but did prevent an hCG-stimulated increase in proliferation (Figure 4C). Similarly, the phospholipase C inhibitor U73122 did not alter proliferation but did prevent hCG-stimulated proliferation (Figure 4D).

LH stimulation of LHCGR in mOMECs

Additional studies demonstrated that recombinant human LH at concentrations of 20 and 200 IU/mL also increased media cAMP (Figure 5A) and mOMEC proliferation as assessed by Ki67 immunodetection (Figure 5B).

Functional LHCGRs in hOMECs

hOMECs were also evaluated to determine if functional LHCGRs were present in endothelial cells of human ovulatory follicles. *LHCGR* (Figure 6A) was detected in hOMECs by nested PCR. Treatment of hOMECs with 20 IU/mL hCG stimulated hOMEC migration (Figure 6B) and proliferation (Figure 6C).

Discussion

The present report identifies LHCGR mRNA and protein in vascular endothelial cells of primate ovulatory follicles. LHCGR expression in granulosa and theca cells is first observed at the secondary follicle stage and is consistently detected throughout subsequent follicle growth in rodents, monkeys, and women [13, 14, 31, 32]. LHCGR expression in granulosa cells is high prior to the ovulatory gonadotropin surge and decreases after surge [13, 14, 31, 32]. In contrast, LHCGR mRNA and protein expression by cumulus granulosa cells and oocytes is low to nondetectable throughout the ovulatory interval [13, 14]. In our study, mural granulosa cells of large macaque preovulatory follicles show high levels of LHCGR mRNA and protein prior to the LH surge, with decreased detection after the surge, similar to these prior reports [13, 14, 31, 32]. Monkey theca cells also expressed LHCGR mRNA and protein in vitro as anticipated. Generally, mural granulosa and theca cells are considered the primary targets for LH action in the dominant follicle prior to ovulation [1]. We considered that our mOMEC populations may contain small numbers of LHCGR-expressing granulosa or theca cells, resulting in the detection of LHCGR mRNA and protein. However, mOMECs did not contain CYP17A1 or CYP19A1 positive cells by immunostaining, and all mOMECs showed LHCGR by immunostaining. Importantly, we detected LHCGR in ovarian follicular vascular endothelial cells both in vitro and in vivo. It is interesting to note that LHCGR was not detected by immunostaining in vascular endothelial cells of the corpus luteum or larger ovarian vessels of the ovarian stroma. This observation supports the hypothesis that LHCGR-driven angiogenesis within the ovary

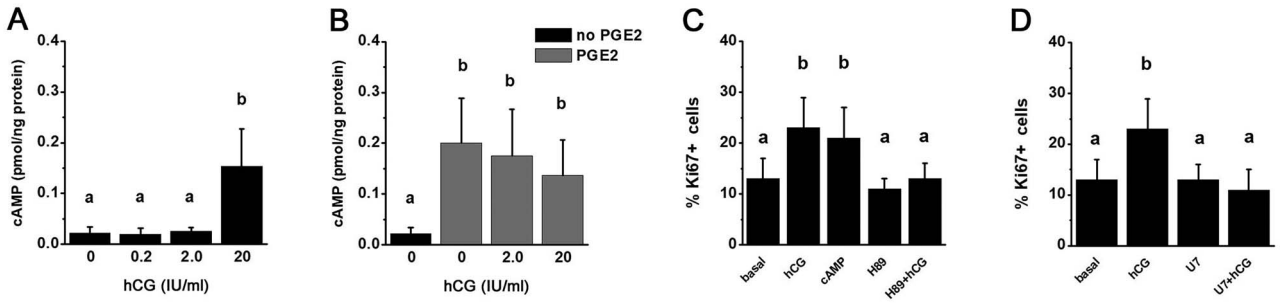

Figure 4. hCG-activated signaling pathways in mOMECs. (A)–(B) mOMECs treated with hCG (0, 0.2, 2.0, 20 IU/ml) without or with PGE2 (1 μM; grey bars) were assessed for cAMP accumulation in culture media (A, $n=5$ mOMEC lines; B, $n=3$ mOMEC lines). cAMP (A, B) was assessed by ELISA and standardized to total cell protein. (C) hCG-stimulated proliferation after treatment for 24 h with dibutyryl cAMP (10 mM), hCG (20 IU/mL), and/or the protein kinase A inhibitor H89 (1 μM; $n=3$ mOMEC lines). (D) hCG-stimulated proliferation after no treatment (basal), treatment with hCG (20 IU/mL), and/or treatment with the phospholipase C inhibitor U71322 (U7, 1 μM; $n=3$ mOMEC lines). Proliferation (C, D) was assessed by Ki67 immunodetection and expressed as the percentage of total cells that are Ki67 positive. For each panel, groups with different letters are different, $P<0.05$ by ANOVA with one repeated measure.

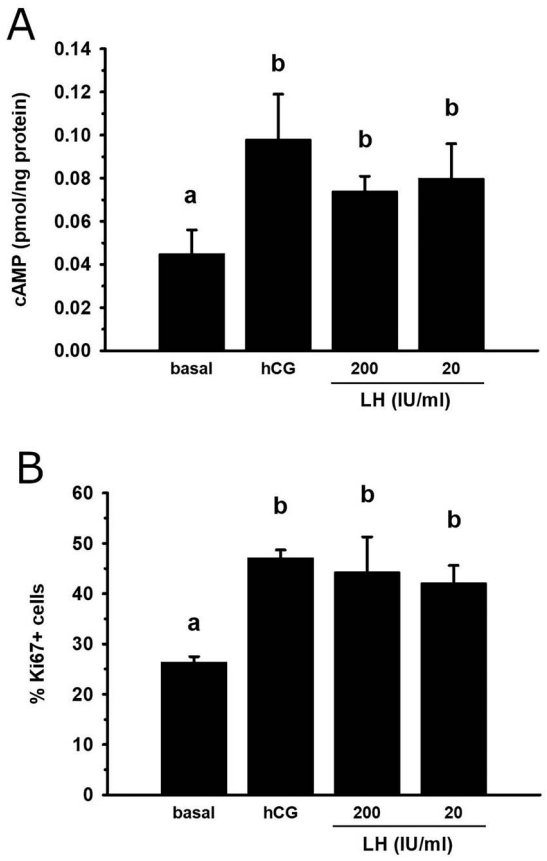

Figure 5. LH activates LHCGR in mOMECs. (A) mOMECs in basal media or basal media with hCG (20 IU/mL) or LH (20 or 200 IU/mL) were assessed for cAMP accumulation in media; cAMP was assessed by ELISA and standardized to total cell protein. $n=4$ mOMEC lines. (B) hCG (20 IU/mL) and LH (20 or 200 IU/mL) increase mOMEC proliferation over the basal medium ($n=3$ mOMEC lines). For each panel, groups with different letters are different, $P<0.05$ by ANOVA with one repeated measure.

may be limited to the ovulatory follicle. Overall, our findings add the vascular endothelial cell of the ovulatory follicle to the list of follicular cell types capable of responding directly to LH.

There is compelling evidence that LHCGR mRNA and protein are expressed by many types of cells, including vascular endothelial cells, within and beyond the reproductive system. Gonads are traditional targets for LH/hCG action. Steroidogenic cells of the primate corpus luteum express LHCGR; they respond to LH during the reproductive cycle and to chorionic gonadotropin (CG) in early pregnancy [33]. Leydig cells of the testis respond to LH via LHCGR [34]. In addition, the endometrium responds directly to CG secreted by the embryo at the time of implantation [35]. Prior reports show that human umbilical vein endothelial cells (HUVECs) and both endothelial and epithelial cells of the uterine endometrium express LHCGR and respond to LHCGR stimulation [17, 18]. LHCGR mRNA and protein have also been reported in tissues outside the reproductive tract. The cortical cells of the adrenal gland express LHCGR, perhaps because of a common embryological origin with the gonads [36]. LHCGRs on adrenal cortical cells have been implicated in altered adrenal function in polycystic ovary syndrome, pregnancy, and adrenal cortical neoplasms [36]. The fetal retina expresses LHCGR, and stimulation of these LHCGRs has been implicated in mouse eye development [37]. Human lymphatic endothelial cells and circulating angiogenic progenitor cells have also been shown to express LHCGR [19]. The wide distribution of LHCGRs within and beyond the reproductive tissues suggest multiple functions for this receptor and its ligands, LH and CG.

Regulation of LHCGR is complex. In the present study, administration of hCG in vivo led to decreased LHCGR mRNA and protein in follicular granulosa cells. In contrast, LHCGR immunodetection in mOMECs persisted after hCG treatment in vivo and in vitro. LH or CG binding to the LHCGR can reduce receptor numbers via a variety of mechanisms (reviewed in [38]). Interestingly, hCG treatment of mOMECs and monkey theca cells in vitro led to a shift in cellular location of LHCGR, with a concentration of LHCGR detected near the nucleus after hCG exposure. This ligand-driven response is consistent with LHCGR internalization reported for other LH/CG-responsive cells [39–41]. Regulation of LHCGR mRNA and protein by other mechanisms has been reported. In mouse granulosa and theca cells, *LHCGR* correlates with methylation status of the LHCGR promoter, where demethylation leads to enhanced *LHCGR* in granulosa cells of preovulatory follicles [42]. A primary endocrine regulator of LHCGR is FSH, which increases *LHCGR* in granulosa cells of preovulatory follicles [43]. This mechanism may be most important for preovulatory granulosa cells, as

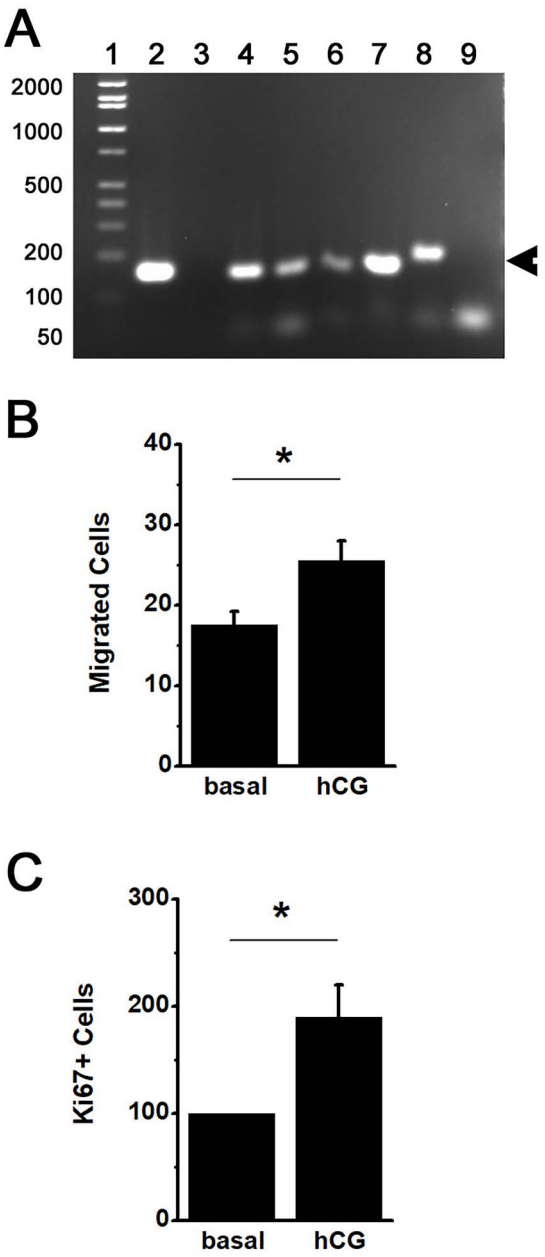

Figure 6. LHCGR expression and function in hOMECs. (A) LHCGR mRNA was detected in hOMECs by nested PCR. Molecular size standards (base pairs, lane 1) are shown at the left. Nested LHCGR cDNA amplified fragment (163 bp) shown at arrow (right). Sample lanes show amplification of cDNA from (2) LHCGR standard, (3) no cDNA control (water), (4) monkey granulosa cells, (5–8) re-amplified first round PCR cDNA from individual hOMEC lines ($n = 4$), (9) re-amplified no cDNA control from the first round PCR. (B) hCG-stimulated migration. hCG increases the number of migrated cells when compared with the basal medium alone, $n = 4$ hOMEC lines. (C) hCG increases hOMEC proliferation over the basal medium alone. For each hOMEC line, basal proliferation set equal to 100%, and hCG-stimulated proliferation expressed relative to the basal level. $n = 4$ hOMEC lines. In (B) and (C), significant differences were detected by the paired t-test, $P < 0.05$, as indicated by the asterisk (*).

FSH receptors (FSHR) are expressed predominantly by this follicular cell type. HUVECs also express FSHR [44], so FSH-induced increase in *LHCGR* may occur in tissues other than the ovarian follicle. The involvement of FSHR signaling and *LHCGR* promoter methylation in the regulation of LHCGR mRNA and protein in mOMECs or hOMECs has yet to be examined.

LHCGR stimulation promoted angiogenic actions in mOMECs in vitro, including migration, proliferation, and capillary sprout formation. Migration of an endothelial tip cell, followed by proliferating endothelial cells to form a tube lumen, are essential components of the formation of a new capillary [27]. In the present study, hCG promoted these angiogenic actions in vitro. For example, hCG treatment resulted in a 2-fold increase (over basal levels) in migration in mOMECs and a 1.7-fold increase in migration in hOMECs. This is similar to our prior studies of VEGFA-stimulated migration, where VEGFA treatment resulted in a 2-fold increase in migration for both mOMECs [45] and hOMECs [21] in vitro. In studies of other types of endothelial cells, hCG was also as effective as VEGFA to promote migration, proliferation, and sprout formation [18, 46]. A wide variety of in vitro and in vivo models have been used to support the concept that hCG acts directly at endothelial cells to stimulate angiogenesis at concentrations similar to those used in our present study [17–19]. Whereas our studies focus specifically on angiogenesis in the ovarian follicle at the time of ovulation, there is ample evidence that hCG, at ovulatory concentrations, may be a potent pro-angiogenic stimulus in many organs.

In the present study, both hCG and LH at 20 IU/mL resulted in similar stimulation of mOMEC cAMP and proliferation. Concentrations of hCG and LH used in the present study have previously been shown to stimulate changes in granulosa cells in vitro consistent with changes observed after administration of an ovulatory dose of hCG in vivo for collection of mature oocyte for in vitro fertilization. For example, hCG at a dose of 20 IU/mL in vitro was shown to regulate monkey granulosa cell prostaglandin synthesis/metabolism [47, 48], cell cycle [49, 50], and epidermal growth factor like ligands [51]. LH is used less frequently in vitro, but LH stimulation of ovulatory changes in granulosa cell cultures has been reported [52]. Taken together, these findings indicate that mOMECs respond to an ovulatory dose of LHCGR ligand with angiogenic changes.

LHCGRs expressed by mOMECs utilize previously reported signal transduction pathways [29]. Previous studies have identified the Gαs protein as a key mediator of LHCGR activation [22–24]. LHCGRs in mOMECs also utilize the Gαs–cAMP–PKA pathway. For example, we demonstrated that dibutyryl cAMP mimicked the ability of hCG to increase proliferation, while inhibition of PKA with H89 [53] blocked hCG-stimulated proliferation. Other G proteins have also been linked to LHCGR activation. Davis et al. [54] showed that inositol triphosphate levels increased in rat granulosa cells in response to LH, and selective deletion of Gαq/11 in mouse granulosa cells impaired generation of inositol phosphates, progesterone production, and ovulation [30]. In our studies of mOMECs, U71322 blocked hCG-stimulated proliferation. U71322 is widely accepted as an inhibitor of phospholipase C [55], implicating Gαq as a mediator of LHCGR stimulation, but alternative targets for U71322 have been suggested [56]. Our initial studies reported here focused on traditional LHCGR signaling pathways. Additional signaling pathways have been implicated in mediation of hCG action [16, 57] and may also be involved in LH/hCG-stimulated angiogenesis in the ovulatory follicle.

Data presented in this manuscript support the intriguing suggestion that the midcycle LH surge promotes ovulatory angiogenesis via multiple mechanisms. Many vascular growth factors are produced within the ovulatory follicle in response to the LH surge, and these growth factors promote healthy ovulatory angiogenesis (reviewed in [1]). Furthermore, LH action at granulosa and theca contributes to breakdown of the granulosa cell basal lamina and, more generally, remodeling of the extracellular matrix [58, 59]; this reorganization of extracellular matrix provides focal areas conducive to capillary penetration into the granulosa cell layer, which facilitates new vessel formation (reviewed in [1]). In addition, we propose that LHCGR stimulation may directly promote the rapid angiogenesis, which occurs as the follicle moves toward ovulation and transformation into the corpus luteum. A growing body of work suggests a causal relationship between follicular angiogenesis and successful release of the oocyte at ovulation [5, 8, 10, 45, 60]. In each of these studies, disruption of angiogenic factor action resulted in reduced or absent ovulation. Further experiments will be necessary to discern the individual contributions made by direct action of LH at the LHCGR and other LH-regulated processes to the overall success of ovulatory angiogenesis and, ultimately, ovulation in primates, including monkeys and women.

Author contributions

ML planned and conducted experiments, drafted and edited the manuscript, and approved the final manuscript; ACP planned and conducted experiments, edited the manuscript, and approved the final manuscript; MAGS planned and conducted experiments, edited the manuscript, and approved the final manuscript; DMD obtained funding, planned and conducted experiments, edited the manuscript, and approved the final manuscript.

Supplementary material

Supplementary material is available at *BIOLRE* online.

Data availability

There are no data sets associated with this manuscript.

Acknowledgments

Dr Asgerally Fazleabas generously supplied the LHCGR antibody used in these studies. Recombinant human FSH and Ganirelix were generously provided by the Investigator-Initiated Studies Program of Organon (Jersey City, NJ). The opinions expressed in this paper are those of the authors and do not necessarily represent those of Organon.

Conflict of interest

The authors have declared that no conflict of interest exists.

References

1. Duffy DM, Ko C, Jo M, Brannstrom M, Curry TE. Ovulation: parallels with inflammatory processes. *Endocr Rev* 2019; **40**: 369–416.
2. Stouffer RL, Martinez-Chequer JC, Molskness TA, Xu F, Hazzard TM. Regulation and action of angiogenic factors in the primate ovary. *Arch Med Res* 2001; **32**:567–575.
3. Hibbert ML, Stouffer RL, Wolf DP, Zelinski-Wooten MB. Midcycle administration of a progesterone synthesis inhibitor prevents ovulation in primates. *Proc Natl Acad Sci USA* 1996; **93**: 1897–1901.
4. Acosta TJ, Miyamoto A. Vascular control of ovarian function: ovulation, corpus luteum formation and regression. *Anim Reprod Sci* 2004; **82-83**:127–140.
5. Trau HA, Davis JS, Duffy DM. Angiogenesis in the primate ovulatory follicle is stimulated by luteinizing hormone via prostaglandin E2. *Biol Reprod* 2015; **92**:15.
6. Wong WYL, Richards JS. Evidence for two antigenically distinct molecular weight variants of prostaglandin H synthase in the rat ovary. *Mol Endocrinol* 1991; **5**:1269–1279.
7. Hazzard TM, Molskness TA, Chaffin CL, Stouffer RL. Vascular endothelial growth factor (VEGF) and angiopoietin regulation by gonadotrophin and steroids in macaque granulosa cells during the peri-ovulatory interval. *Mol Hum Reprod* 1999; **5**:1115–1121.
8. Bender HR, Trau HA, Duffy DM. Placental growth factor is required for ovulation, luteinization, and angiogenesis in primate ovulatory follicles. *Endocrinology* 2018; **159**:710–722.
9. Koos RD. Increased expression of vascular endothelial growth/permeability factory in the rat ovary following an ovulatory stimulus: potential roles in follicle rupture. *Biol Reprod* 1995; **52**: 1426–1435.
10. Bender HR, Campbell GE, Aytoda P, Mathiesen AH, Duffy DM. Thrombospondin 1 (THBS1) promotes follicular angiogenesis, luteinization, and ovulation in primates. *Front Endocrinol (Lausanne)* 2019; **10**:727.
11. Berisha B, Schams D, Rodler D, Sinowatz F, Pfaffl MW. Expression and localization of members of the thrombospondin family during final follicle maturation and corpus luteum formation and function in the bovine ovary. *J Reprod Dev* 2016; **62**:501–510.
12. Miyabayashi K, Shimizu T, Kawauchi C, Sasada H, Sato E. Changes of mRNA expression of vascular endothelial growth factor, angiopoietins and their receptors during the periovulatory period in eCG/hCG-treated immature female rats. *J Exp Zool A Comp Exp Biol* 2005; **303**:590–597.
13. Peng XR, Hsueh AJ, LaPolt PS, Bjersing L, Ny T. Localization of luteinizing hormone receptor messenger ribonucleic acid expression in ovarian cell types during follicle development and ovulation. *Endocrinology* 1991; **129**:3200–3207.
14. Yung Y, Aviel-Ronen S, Maman E, Rubinstein N, Avivi C, Orvieto R, Hourvitz A. Localization of luteinizing hormone receptor protein in the human ovary. *Mol Hum Reprod* 2014; **20**: 844–849.
15. Baena V, Owen CM, Uliasz TF, Lowther KM, Yee SP, Terasaki M, Egbert JR, Jaffe LA. Cellular heterogeneity of the luteinizing hormone receptor and its significance for cyclic GMP signaling in mouse preovulatory follicles. *Endocrinology* 2020; **161**:1–18.
16. Bourdiec A, Bedard D, Rao CV, Akoum A. Human chorionic gonadotropin regulates endothelial cell responsiveness to interleukin 1 and amplifies the cytokine-mediated effect on cell proliferation, migration and the release of angiogenic factors. *Am J Reprod Immunol* 2013; **70**:127–138.
17. Berndt S, Perrier d'Hauterive S, Blacher S, Pequeux C, Lorquet S, Munaut C, Applanat M, Herve MA, Lamande N, Corvol P, van den Brule F, Frankenne F *et al.* Angiogenic activity of human chorionic gonadotropin through LH receptor activation on endothelial and epithelial cells of the endometrium. *FASEB J* 2006; **20**:2630–2632.
18. Zygmunt M, Herr F, Keller-Schoenwetter S, Kunzi-Rapp K, Munstedt K, Rao CV, Lang U, Preissner KT. Characterization of human chorionic gonadotropin as a novel angiogenic factor. *J Clin Endocrinol Metab* 2002; **87**:5290–5296.
19. Schanz A, Lukosz M, Hess AP, Baston-Bust DM, Krussel JS, Heiss C. hCG stimulates angiogenic signals in lymphatic endothelial and circulating angiogenic cells. *J Reprod Immunol* 2015; **110**: 102–108.
20. Seachord CL, VandeVoort CA, Duffy DM. Adipose-differentiation related protein: a gonadotropin- and prostaglandin-regulated

protein in primate periovulatory follicles. *Biol Reprod* 2005; **72**: 1305–1314.
21. Trau HA, Brannstrom M, Curry TEJ, Duffy DM. Prostaglandin E2 and vascular endothelial growth factor A mediate angiogenesis of human ovarian follicular endothelial cells. *Hum Reprod* 2016; **31**: 436–444.
22. Duffy DM, Seachord CL, Dozier BL. Microsomal prostaglandin E synthase-1 (mPGES-1) is the primary form of PGES expressed by the primate periovulatory follicle. *Hum Reprod* 2005; **20**: 1485–1492.
23. McAllister JM, Kerin JFP, Trant JM, Estabrook RW, Mason JI, Waterman MR, Simpson ER. Regulation of cholesterol side-chain cleavage and 17α-hydroxylase/lyase activities in proliferating human theca interna cells in long term monolayer culture. *Endocrinology* 1989; **125**:1959–1966.
24. Cameo P, Szmidt M, Strakova Z, Mavrogianis P, Sharpe-Timms KL, Fazleabas AT. Decidualization regulates the expression of the endometrial chorionic gonadotropin receptor in the primate. *Biol Reprod* 2006; **75**:681–689.
25. Markosyan N, Dozier BL, Lattanzio FA, Duffy DM. Primate granulosa cell response via prostaglandin E2 receptors increases late in the periovulatory interval. *Biol Reprod* 2006; **75**:868–876.
26. Duffy DM, Stouffer RL. Progesterone receptor messenger ribonucleic acid in the primate corpus luteum during the menstrual cycle: possible regulation by progesterone. *Endocrinology* 1995; **136**: 1869–1876.
27. Herbert SP, Stainier DYR. Molecular control of endothelial cell behaviour during blood vessel morphogenesis. *Nat Rev* 2011; **12**: 551–564.
28. Molskness TA, Zelinski-Wooten MB, Hild-Petito SA, Stouffer RL. Comparison of the steroidogenic response of luteinized granulosa cells from rhesus monkeys to luteinizing hormone and chorionic gonadotropin. *Biol Reprod* 1991; **45**:273–281.
29. McFarland KC, Sprengel R, Phillips HS, Kohler M, Rosemblit N, Nikolics K, Segaloff DL, Seeburg PH. Lutropin-choriogonadotropin receptor: an unusual member of the G protein-coupled receptor family. *Science* 1989; **245**:494–499.
30. Breen SM, Andric N, Ping T, Xie F, Offermans S, Gossen JA, Ascoli M. Ovulation involves the luteinizing hormone-dependent activation of G(q/11) in granulosa cells. *Mol Endocrinol* 2013; **27**: 1483–1491.
31. Park OK, Mayo KE. Transient expression of progesterone receptor messenger RNA in ovarian granulosa cells after the preovulatory luteinizing hormone surge. *Mol Endocrinol* 1991; **5**:967–978.
32. Xu F, Stouffer RL, Muller J, Hennebold JD, Wright JW, Bahar A, Leder G, Peters M, Thorne M, Sims M, Wintermantel T, Lindenthal B. Dynamics of the transcriptome in the primate ovulatory follicle. *Mol Hum Reprod* 2011; **17**:152–165.
33. Przygrodzka E, Plewes MR, Davis JS. Luteinizing hormone regulation of inter-organelle communication and fate of the corpus luteum. *Int J Mol Sci* 2021; **22**:9972.
34. Saez JM. Leydig cells: endocrine, paracrine, and autocrine regulation. *Endocr Rev* 1994; **15**:574–626.
35. Gridelet V, Perrier d'Hauterive S, Polese B, Foidart JM, Nisolle M, Geenen V. Human chorionic gonadotrophin: new pleiotropic functions for an "Old" hormone during pregnancy. *Front Immunol* 2020; **11**:343.
36. Bernichtein S, Alevizaki M, Huhtaniemi I. Is the adrenal cortex a target for gonadotropins? *Trends Endocrinol Metab* 2008; **19**: 231–238.
37. Movsas TZ, Sigler R, Muthusamy A. Elimination of signaling by the luteinizing hormone receptor reduces ocular VEGF and retinal vascularization during mouse eye development. *Curr Eye Res* 2018; **43**:1286–1289.
38. Menon KM, Menon B. Structure, function and regulation of gonadotropin receptors - a perspective. *Mol Cell Endocrinol* 2012; **356**:88–97.
39. Lamm ML, Hunzicker-Dunn M. Phosphorylation-independent desensitization of the luteinizing hormone/chorionic gonadotropin receptor in porcine follicular membranes. *Mol Endocrinol* 1994; **8**:1537–1546.
40. Hipkin RW, Liu X, Ascoli M. Truncation of the C-terminal tail of the follitropin receptor does not impair the agonist- or phorbol ester-induced receptor phosphorylation and uncoupling. *J Biol Chem* 1995; **270**:26683–26689.
41. Nair AK, Peegel H, Menon KM. The role of luteinizing hormone/human chorionic gonadotropin receptor-specific mRNA binding protein in regulating receptor expression in human ovarian granulosa cells. *J Clin Endocrinol Metab* 2006; **91**:2239–2243.
42. Kawai T, Richards JS, Shimada M. The cell type-specific expression of LHCGR in mouse ovarian cells: evidence for a DNA-demethylation-dependent mechanism. *Endocrinology* 2018; **159**: 2062–2074.
43. LaPolt PS, Oikawa M, Jia XC, Dargan C, Hsueh AJ. Gonadotropin-induced up- and down-regulation of rat ovarian LH receptor message levels during follicular growth, ovulation and luteinization. *Endocrinology* 1990; **126**:3277–3279.
44. Stilley JA, Guan R, Duffy DM, Segaloff DL. Signaling through FSH receptors on human umbilical vein endothelial cells promotes angiogenesis. *J Clin Endocrinol Metabol* 2014; **99**: E813–E820.
45. Kim SO, Trau HA, Duffy DM. Vascular endothelial growth factors C and D may promote angiogenesis in the primate ovulatory follicle. *Biol Reprod* 2017; **96**:389–400.
46. Herr F, Baal N, Reisinger K, Lorenz A, McKinnon T, Preissner KT, Zygmunt M. HCG in the regulation of placental angiogenesis. Results of an in vitro study. *Placenta* 2007; **28** Suppl A:S85–S93.
47. Duffy DM, Dozier BL, Seachord CL. Prostaglandin dehydrogenase and prostaglandin levels in periovulatory follicles: implications for control of primate ovulation by PGE2. *J Clin Endocrinol Metabol* 2005; **90**:1021–1027.
48. Duffy DM, Seachord CL, Dozier BL. An ovulatory gonadotropin stimulus increases cytosolic phospholipase A2 (cPLA2) expression and activity in granulosa cells of primate periovulatory follicles. *J Clin Endocrinol Metabol* 2005; **90**:5858–5865.
49. Fru KN, VandeVoort CA, Chaffin CL. Mineralocorticoid synthesis during the periovulatory interval in macaques. *Biol Reprod* 2006; **75**:568–574.
50. Chaffin CL, Brogan RS, Stouffer RL, VandeVoort CA. Dynamics of Myc/Max/Mad expression during luteinization of primate granulosa cells in vitro: association with periovulatory proliferation. *Endocrinology* 2003; **144**:1249–1256.
51. Puttabyatappa M, Brogan RS, Vandevoort CA, Chaffin CL. EGF-like ligands mediate progesterone's anti-apoptotic action on macaque granulosa cells. *Biol Reprod* 2013; **88**:18.
52. Duffy DM, Stouffer RL. Luteinizing hormone acts directly at granulosa cells to stimulate periovulatory processes: modulation of luteinizing hormone effects by prostaglandins. *Endocrine* 2003; **22**:249–256.
53. Takuma T, Ichida T. Evidence for the involvement of protein phosphorylation in cyclic AMP-mediated amylase exocytosis from parotid acinar cells. *FEBS Lett* 1994; **340**:29–33.
54. Davis JS, Weakland LL, West LA, Farese RV. Luteinizing hormone stimulates the formation of inositol trisphosphate and cyclic AMP in rat granulosa cells. Evidence for phospholipase C generated second messengers in the action of luteinizing hormone. *Biochem J* 1986; **238**:597–604.
55. Bleasdale JE, Thakur NR, Gremban RS, Bundy GL, Fitzpatrick FA, Smith RJ, Bunting S. Selective inhibition of receptor-coupled phospholipase C-dependent processes in human platelets and polymorphonuclear neutrophils. *J Pharmacol Exp Ther* 1990; **255**: 756–768.
56. Leitner MG, Michel N, Behrendt M, Dierich M, Dembla S, Wilke BU, Konrad M, Lindner M, Oberwinkler J, Oliver D. Direct modulation of TRPM4 and TRPM3 channels by the phospholipase C inhibitor U73122. *Br J Pharmacol* 2016; **173**:2555–2569.
57. Berndt S, Blacher S, Munaut C, Detilleux J, Perrier d'Hauterive S, Huhtaniemi I, Evain-Brion D, Noel A, Fournier T, Foidart

JM. Hyperglycosylated human chorionic gonadotropin stimulates angiogenesis through TGF-beta receptor activation. *FASEB J* 2013; **27**:1309–1321.
58. Irving-Rodgers HF, Catanzariti KD, Aspden WJ, D'Occhio MJ, Rodgers RJ. Remodeling of extracellular matrix at ovulation of the bovine ovarian follicle. *Mol Reprod Dev* 2006; **73**: 1292–1302.
59. Irving-Rodgers HF, Hummitzsch K, Murdiyars LS, Bonner WM, Sado Y, Nimomiya Y, Couchman JR, Sorokin LM, J. RR. Dynamics of extracellular matrix in ovarian follicles and corpora lutea of mice. *Cell Tissue Res* 2010; **339**:613–624.
60. Campbell GE, Bender HR, Parker GA, Curry TE Jr, Duffy DM. Neurotensin: a novel mediator of ovulation? *FASEB J* 2021; **35**:e21481.